Optimal reactive power dispatch of permanent magnet synchronous generator-based wind farm considering levelised production cost minimisation

Li, Jian; Wang, Ni; Zhou, Dao; Hu, Weihao; Huang, Qi; Chen, Zhe; Blaabjerg, Frede

Published in:
Renewable Energy

DOI (link to publication from Publisher):
10.1016/j.renene.2019.06.014

Publication date:
2020

Document Version
Accepted author manuscript, peer reviewed version

Accepted Manuscript

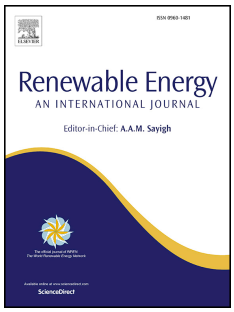

Optimal reactive power dispatch of permanent magnet synchronous generator-based wind farm considering levelised production cost minimisation

Jian Li, Ni Wang, Dao Zhou, Weihao Hu, Qi Huang, Zhe Chen, Frede Blaabjerg

PII: S0960-1481(19)30827-4

DOI: https://doi.org/10.1016/j.renene.2019.06.014

Reference: RENE 11746

To appear in: *Renewable Energy*

Received Date: 4 March 2019

Revised Date: 30 May 2019

Accepted Date: 3 June 2019

Please cite this article as: Li J, Wang N, Zhou D, Hu W, Huang Q, Chen Z, Blaabjerg F, Optimal reactive power dispatch of permanent magnet synchronous generator-based wind farm considering levelised production cost minimisation, *Renewable Energy* (2019), doi: https://doi.org/10.1016/j.renene.2019.06.014.

Optimal Reactive Power Dispatch of Permanent Magnet Synchronous Generator-Based Wind Farm Considering Levelised Production Cost Minimisation

Jian Li[1], Ni Wang[1], Dao Zhou[2], Weihao Hu[1,*], Qi Huang[1], Zhe Chen[2], Frede Blaabjerg[2]

[1]School of Mechanical and Electrical Engineering, University of Electronic Science and Technology of China, Chengdu, China
[2]Department of Energy Technology, Aalborg University, Aalborg, Denmark
leejian@uestc.edu.cn, wangni@std.uestc.edu.cn, zda@et.aau.dk, whu@uestc.edu.cn, hwong@uestc.edu.cn, zch@et.aau.dk, fbl@et.aau.dk

[*]Author to whom correspondence should be addressed; E-Mail: whu@uestc.edu.cn; Tel.: +86-183-0280-9968

Abstract: As wind power penetration increases, large wind farms (WFs) need to provide reactive power according to modern grid codes. Permanent magnet synchronous generator-based wind turbines (WTs) can generate reactive power, by assigning the appropriate reactive power to each WT to meet the reactive power requirements of the grid. This is a more economical method than setting up additional reactive power compensation equipment. This study proposes an optimal reactive power dispatch strategy for minimising a levelised production cost, and is implemented in two ways: minimising the power loss of a WF, and maximising the lifetime of WTs. The reactive power references of each WT are chosen as the optimisation variables, and a particle swarm optimisation algorithm is adopted to solve the optimisation problem. The proposed and traditional reactive power dispatch strategies are demonstrated and compared on a WF with 25 WTs to validate the effectiveness of the proposed approach.

***Index Terms*—Reactive power dispatch, permanent magnet synchronous generator, power loss, lifetime, levelised production cost.**

Nomenclature

u_{sd}	d-axis voltage of stator	R_{IGBT}	the resistance of the insulated-gate bipolar transistor (IGBT)
u_{sq}	q-axis voltage of stator	R_{filter}	resistance of the filter
R_s	resistance of generator	I_{gd}	d-axis current of the grid side converter
i_{sd}	d-axis current of stator	I_{gq}	q-axis current of the grid side converter
i_{sq}	q-axis current of stator	P_0	no-load loss of transformer
L_s	inductance of generator	P_k	load loss of transformer
ψ	flux of permanent magnet	β	the load ratio
ω_e	electrical rotating speed of generator	C_0	present value of the capital cost
ω_g	mechanical rotating speed of generator	CAP_t	capital cost in year *t*.
n_p	number of pole pairs	r	the discount ratio

$\lvert I_s \rvert$	root mean square value of stator phase current	N_y	lifetime
k_1	a constant describes iron losses at rated speed	E_{tol}	energy yield in one year
I_{rms}	root mean square value of the current at converter AC terminal	v_i^k	velocity of particle *i* at *k*-th iteration
V_{IGBT}	voltage across the collector and emitter of the IGBT	x_i^k	position of particle *i* at *k*-th iteration
f_{sw}	switching frequency	c_1, c_2	acceleration coefficients
$I_{C,nom}$	nominal collector current of IGBT	r_1, r_2	random numbers between 0 and 1
E_{on}	the turn-on energies of IGBT	$pbest_i^k$	personal best position of particle *i* at *k*-th iteration
E_{off}	the turn-off energies of IGBT	$gbest^k$	global best position at *k*-th iteration
E_{rr}	turn-off energy of the diode		

1. Introduction

Wind power technology has developed rapidly in recent years. The installed capacity of wind power increased by 51.3 GW in 2018, bringing the global total installed capacity to 591 GW. The Global Wind Energy Council forecasts that the sector will return to rapid growth in 2019, and move upwards to reach a total installed capacity of 840 GW by 2022 [1]. This development in wind energy brings increasing wind penetration levels into the grid. In Denmark, 44% of the electricity in 2017 was obtained from wind power [2]. However, the fluctuation of wind speed and the errors in wind resource prediction bring additional uncertainty regarding wind energy [3]. Moreover, the uncertainty of wind power brings variability into operational planning [4]. In addition, the high percentage of wind penetration may affect the stability of the power grid [5]. Thus, grid codes require that wind farms (WFs) should be able to provide reactive power to support a grid voltage [6].

To provide the reactive power needed by the grid, most WFs are equipped with some fast volt-ampere reactive (var) regulation devices, such as capacitor banks, static synchronous compensators (STATCOMs), and static var compensators (SVCs) [7]–[8]. In fact, a grid-side converter (GSC) inside a doubly-fed induction generator (DFIG) wind turbine (WT) or a permanent magnet synchronous generator (PMSG) WT has the ability to control the reactive power and voltage [9]. As a result, in large-scale WFs constructed with DFIGs or PMSGs, each WT can be seen as a reactive power source. By assigning an appropriate reactive reference to each WT, the reactive power at the point of common coupling (PCC) can meet the requirements of the power grid.

A reactive power dispatch strategy aims to allocate the total reactive power needed at the PCC to each WT inside the WF. The traditional strategy is a proportional dispatch strategy, in which each WT's reactive power reference is allocated according to its available reactive power capacity [10]. This method is easy to implement with a small number of calculations. However, considering the stochastic nature of wind and the increasing penetration of wind power generation, this reactive power dispatch is no longer suitable for large-scale WFs. Much research has been devoted to various reactive power dispatch strategies based on different objective functions to meet different operation requirements of a WF, including lower active power loss [11] –[13], higher power quality [14]–[16], and higher reliability [17]–[20]. Reference [21] adopts a genetic algorithm to obtain a coordinated reactive power management among DFIG WTs and SVCs to improve the voltage stability. Reference [22] proposes a reactive power assignment plan for a SVC-based WF, which can maximise the reactive power reserve and minimise the system loss. Reference [23] uses both WTs and SVCs as the reactive power source to realise a WF low-voltage ride through (LVRT) capability. Reference [24] considers five operating modes to examine the reactive power strategies of a DFIG WT. Reference [25] proposes a multi-objective reactive power strategy to coordinate reactive power among flexible alternating current transmission system (FACTs) devices. Reference [26] considers a wake effect, and proposes a reactive power dispatch method aiming to improve the lifetime of a power converter. Reference [27] comprehensively calculates the active power loss of each part in a WF, and adopts a particle swarm optimisation (PSO) algorithm to minimise the total power loss of the WF. In addition to minimising the loss of the WF, this study also considers the maximum lifetime of the WT. With these two elements as the optimisation goal of this study, an optimisation algorithm is used to find the optimal reactive power allocation strategy for WFs.

When the reactive power command of the WF is given to each WT, the WTs provide extra reactive power in addition to the active power, which may result in a shorter lifetime of the WTs [27]. As mentioned in [28] and [29], the first-commissioned WTs have begun to age, causing a major challenge for the wind industry, and the maintenance cost of offshore WFs cannot be ignored. Thus, it is necessary to consider the lifetime of WTs at a WF under various operation conditions. As described in [30], the lifetime of a WT’s converter is related to the generation of both active power and reactive power. Owing to the wake effect, the WTs at different places may catch different amounts of wind power. One promising way to increase the average lifetime of WTs in a WF is by assigning low reactive power to the WT producing high active power, and assigning high reactive power to the WT producing low active power. Thus, the WF is able to operate for a longer time with a single investment at the beginning, which can reduce the average investment cost.

This study proposes a reactive power dispatch strategy of a PMSG-based WF, aiming to increase the economic benefits of the WF. Both reducing the total power loss of the WF and increasing the lifetime of the WTs can increase the economic benefits of the WF. This study chooses the levelised production cost (LPC) as the objective function, whose value is closely related to both the power loss and the lifetime of the WF. It also adopts a PSO algorithm to determine the reactive power reference of WTs that minimises the LPC of the WF. Finally, the proposed method is implemented in a WF with 25 National Renewable Energy Laboratory (NREL) 5 MW WTs, and the results are compared with a traditional operation strategy.

This paper is organised as follows. Section II describes five loss models present in a WF. Section III introduces a method to calculate the lifetime of a WT. Section IV proposes an improved reactive power dispatch strategy to minimise the LPC. Section V presents a case study, and section VI draws a conclusion.

2. Loss Models inside A Wind Farm

In a wind farm, the main devices are WTs and cables. The PMSG has the advantages of a quick transient response, low maintenance cost, and simple control process [31] [32]. This study takes a PMSG-based WF as an example for analysis. Thus, the WT total power loss consists of five parts of the PMSGs, converters, filters, transformers and cables, and can be expressed as given below:

$$P_{WF}^{loss} = \sum_{k=1}^{n} (P_{PMSG,k}^{loss} + P_{con,k}^{loss} + P_{filter,k}^{loss} + P_{trans,k}^{loss}) + \sum_{l=1}^{m} P_{calbe,l}^{loss} \tag{1}$$

Here, $P_{PMSG,k}^{loss}$ is the loss inside the generator of WT k, $P_{con,k}^{loss}$ is the loss of converter in WT k, $P_{filter,k}^{loss}$ is the loss of filter, $P_{trans,k}^{loss}$ is the loss of transformer of WT k, $P_{calbe,l}^{loss}$ is the loss of cable l, m is the total number of cables, and n is the total number of WTs. The detailed description of each loss model is as follows.

2.1. Permanent Magnet Synchronous Generator (PMSG) Loss Model

The voltage equation and torque equation of PMSG are expressed as [33], [34]

$$\begin{cases} u_{sd} = -R_s i_{sd} + L_s \omega_e i_{sq} \\ u_{sq} = -R_s i_{sq} - L_s \omega_e i_{sd} + \omega_e \psi \end{cases} \tag{2}$$

$$T_e = \frac{3}{2} n_p (\psi_{sd} i_{sq} - \psi_{sq} i_{sd}) \tag{3}$$

The electrical rotating speed of generator ω_e can be given by

$$\omega_e = n_p \omega_g \tag{4}$$

The copper loss inside a PMSG can be calculated by

$$P_{Cu}^{loss} = 3R_s \left| I_s \right|^2 \tag{5}$$

Another loss inside a PMSG is the iron loss, which can be calculated by

$$P_{Fe}^{loss} = k_1 \omega_e \tag{6}$$

In the above, k_1 is a constant for describing the iron losses at a rated speed, and is usually taken as 0.1 [35].

As a result, the power loss of PMSG can be expressed as

$$P_{PMSG}^{loss} = P_{Cu}^{loss} + P_{Fe}^{loss} \tag{7}$$

2.2. Converter Loss Model

As the main components in a converter are the transistors and reverse conduction diodes, their switching and conduction cause power loss. Thus, the loss model of the converter can be calculated as [36]

$$P_{con}^{loss} = a_l I_{rms} + b_l I_{rms}^2 \tag{8}$$

Here, a_l and b_l are the power module constants, and can be expressed as

$$\begin{cases} a_l = \dfrac{6\sqrt{2}}{\pi}\left(V_{IGBT} + \dfrac{E_{on} + E_{off}}{I_{C,nom}} f_{sw} + \dfrac{E_{rr}}{I_{C,nom}} f_{sw} \right) \\ b_l = 3R_{IGBT} \end{cases} \tag{9}$$

In this study, the constants in the equation are chosen as $a_l = 7.0252$, $b_l = 0.0087$, and $f_{sw} = 800$ Hz [27].

2.3. Filter Loss Model

The loss model of filter is expressed as in [27]:

$$P_{filter}^{loss} = R_{filter}(I_{gd}^2 + I_{gq}^2) \tag{10}$$

2.4. Transformer Loss Model

The loss model of the transformer is expressed as in [27]:

$$P_{trans}^{loss} = P_0 + \beta^2 P_k \tag{11}$$

2.5. Cable Loss Model

The cable between bus *i* and bus *j* can be considered as equivalent to the model shown in Fig. 1.

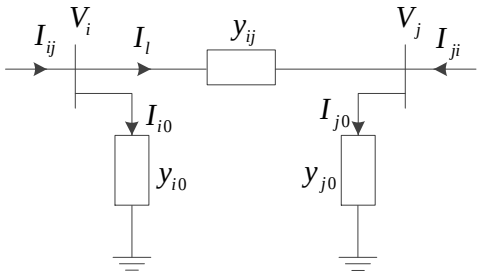

Fig. 1. *Equivalent model of the cable.*

According to the equivalent model in Fig.1, the cable current can be expressed as in [37]:

$$\begin{cases} I_{ij} = I_l + I_{i0} = y_{ij}(V_i - V_j) + y_{i0}V_i \\ I_{ji} = -I_l + I_{j0} = y_{ij}(V_j - V_i) + y_{i0}V_j \end{cases} \tag{12}$$

Thus, the power loss of the cable can be expressed as

$$P_{cable}^{loss} = S_{ij} + S_{ji} = V_i I_{ij}^* + V_j I_{ji}^* \tag{13}$$

In the above, S_{ij} *i*s the complex powers from bus *i* to bus *j*, and S_{ji} is the complex powers from bus *j* to bus *i*.

3. Lifetime of Wind Turbine

For WFs that have been put into operation, especially offshore WFs, the maintenance and repair costs cannot be ignored. Therefore, it is necessary to consider the lifetime of a WT. As previously described, a WT includes a turbine, a gearbox, a generator, and a converter. From the field survey in reference [38], as compared with other parts of the WT, the failure rate of the electrical part of the WT is the highest. Thus, the lifetime of the power converter is the shortest, meaning that the lifetime of the power converter determines the lifetime of the WT. Furthermore, the reactive power dispatch strategy will only affect the lifetime of the converter, but not the WT [39]. Thus, only the lifetime of the converter is evaluated in the following.

Fig. 2 shows a method of estimating the lifetime of a converter in a WT. The input of the model is the active power *P* and the reactive power *Q* of the WT, and the output is the lifetime of the converter in the WT. In the process, the first step is the power converter loading translation, implying that the voltage V_g, current I_g, and phase angle φ_g of the grid-side converter can be calculated through the PMSG model and the converter model. The second step is loss evaluation in the power converter. The loss in the internal components is calculated by the converter loss model, including the IGBT conduction loss, IGBT switching loss, diode conduction loss, and diode switching loss. The third step is the thermal stress evaluation. In this step, a thermal model of the power module is used to evaluate the thermal stress according to the average junction temperature and the junction temperature fluctuation under specific loading conditions, and is closely related to the thermal resistance of the power module and the ambient temperature. Finally, according to the manufacturer's B10 lifetime data under fixed thermal stress, the total endurance power cycle can be calculated by using the Coffin-Manson equation at specific average junction temperatures and junction temperature fluctuations. According to the wind conditions in a year, the annual damage (*AD*) can be derived, and is the reciprocal of the lifetime.

By using this lifetime calculating model, the lifetime of both the grid-side converter and the machine-side converter can be predicted. With respect to a full-scale power converter, a synchronous generator is fully decoupled from the power grid, with the result that the grid-side converter is responsible for the reactive power provision, combined with the active power. Moreover, the thermal loading of the IGBT and the freewheeling diode of the grid-side converter were studied in [40], and it could be seen that the IGBT was much more stressed. As a result, the lifetime of the IGBT in the grid-side converter will be the focus in the following.

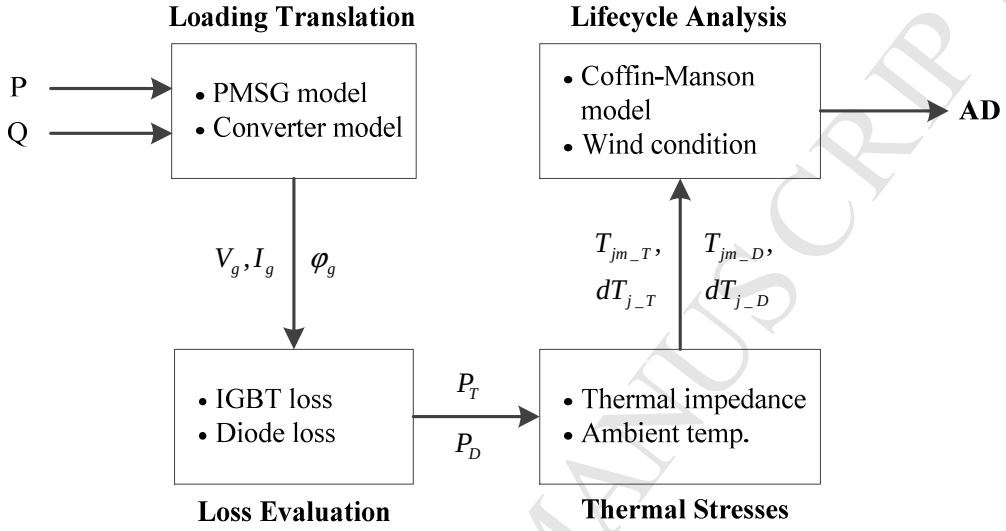

Fig. 2. *Method of estimating the lifetime of the converter*

4. Reactive Power Dispatch Strategy

This section introduces the proposed reactive power dispatch strategy, which aims to find a group of reactive power references of WTs to minimise the LPC of a WF. Thus, the LPC, the objective function and constraints, and the PSO optimisation method are introduced in the following.

4.1. Levelised production cost (LPC)

The LPC is an indicator of the economic benefits of a WF. It considers the cost of capital discounting in the life cycle. The LPC for a WF can be calculated as [41]

$$C_0 = \sum_{t=1}^{N_y} CAP_t (1+r)^t \tag{14}$$

$$LPC = \frac{C_0 r (1+r)^{N_y}}{(1+r)^{N_y} - 1} \frac{1}{E_{tol}} \tag{15}$$

To simplify the calculation, this study only considers a single investment at the beginning.

4.2. Objective function and constrains

In this study, the LPC of a WF is chosen as the objective function. The selection of the LPC as the

objective function can suitably combine the two optimisation factors, i.e. the WF power loss minimisation and the WF lifetime maximisation.

The objective function is given as

$$\min_{Q_{WT,k}^{ref}} \left\{ LPC = \frac{C_0 r(1+r)^{N_y}}{(1+r)^{N_y}-1} \frac{1}{E_{tol}} \right\} \tag{16}$$

$$N_y = \frac{1}{\sum_t^T \left(\frac{1}{N_y^{WF}(t)} * \frac{1}{T} \right)} \tag{17}$$

$$E_{tol} = \sum_{t=1}^{T} \left[\left(\sum_{k=1}^{n} P_{WT,k}(t) - P_{WF}^{loss}(t) \right) * \frac{8760}{T} \right] \tag{18}$$

In the above, T is the number of sampling points in one year, $P_{WT,k}(t)$ is the captured active power of WT k at time t, $P_{WF}^{loss}(t)$ is the power loss of the WF at time t. $N_y^{WF}(t)$ is the lifetime of the WF that can be achieved when the situation at time t is always running, and is limited by the shortest lifetime among the individual WTs, even though the WF can operate with several WTs under forced outages. Moreover, the WTs whose lifetimes reach their maximum inevitably require repair. The increase of the repair cost and the increase of the WTs' lifetime after such repair makes the WF's LPC calculation more complicated, and may require further work for more detailed research and optimisation. Therefore, this study adopts a simplified calculation of LPC, taking the lifetime of the first damaged WT as the lifetime of the WF. Thus, the lifetime of WF can be calculated by Equation (19).

$$N_y^{WF}(t) = \min\{N_y^{WT,k}(t)\}(k = 1, 2, ..., n) \tag{19}$$

Here, $N_y^{WT,k}(t)$ is the lifetime of WT k at time t, and $N_y^{WF}(t)$ is the lifetime of the WF at time t.

The constraints contain the power flow balance limits, the WF reference reactive power constraint, the bus voltage constraint, the GSC current constraint, and the WTs' lifetime limits, and are given as

$$P_j(t) = \left|V_j(t)\right| \sum_{i=1}^{N_B} \left|V_i(t)\right| \left|V_{ji}(t)\right| \cos\left[\theta_{ji}(t) - \delta_j(t) + \delta_i(t)\right] \tag{20}$$

$$Q_j(t) = -\left|V_j(t)\right| \sum_{i=1}^{N_B} \left|V_i(t)\right| \left|V_{ji}(t)\right| \sin\left[\theta_{ji}(t) - \delta_j(t) + \delta_i(t)\right] \tag{21}$$

$$Q_{PCC}(t) = Q_{WF}^{ref}(t) \tag{22}$$

$$V_j^{\min} \le V_j(t) \le V_j^{\max} \tag{23}$$

$$I_{GSC,k}^{rms}(t) \le I_{GSC}^{rated} \tag{24}$$

$$N_y^{WT,k}(t) \le 100 \tag{25}$$

In the above, $P_j(t)$ is the active power injected at bus j at time t, $Q_j(t)$ is the reactive power injected at bus j at time t, $Q_{PCC}(t)$ is the reactive power at the PCC at time t, $Q_{WF}^{ref}(t)$ is the reactive power reference of the WF at time t, $V_j(t)$ is the voltage of bus j at time t, and $I_{GSC,k}^{rms}(t)$ is the root mean square value of the grid side converter current of WT k at time t. The lifetime of WTs is limited to 100 years, as other failure mechanisms may replace the thermal wear-out after such a long operation period.

4.3. Optimisation method

The PSO algorithm was originally introduced by Eberhart and Kennedy, and is suitable for solving non-convex and nonlinear problems [42]. In PSO, each particle has n parameters. First, a group of particles is randomly generated, and is called the first generation. Then, the fitness value of each particle can be calculated by the objective function, denoted by $f\left(x_i(t)\right)$. Up to the present k-th iteration, the optimal position found by particle i is called the personal best position, denoted by $pbest_i^k$, and the optimal position found by all particles is called the global best position, denoted by $gbest^k$. Then, each particle's velocity and position are updated according to $pbest_i^k$ and $gbest^k$, as given below [43]:

$$v_i^{k+1} = v_i^k + c_1 r_1 (pbest_i^k - x_i^k) + c_2 r_2 (gbest^k - x_i^k) \tag{26}$$

$$x_i^{k+1} = v_i^{k+1} + x_i^k \tag{27}$$

In this way, a new generation can be obtained. The same work will be performed on the new generation, until the result is good enough or the number of iterations reaches the maximum.

This study chooses the PSO algorithm to find the appropriate reactive power reference for WTs to minimise the LPC of a WF. The PSO algorithm flowchart is shown in Fig. 3.

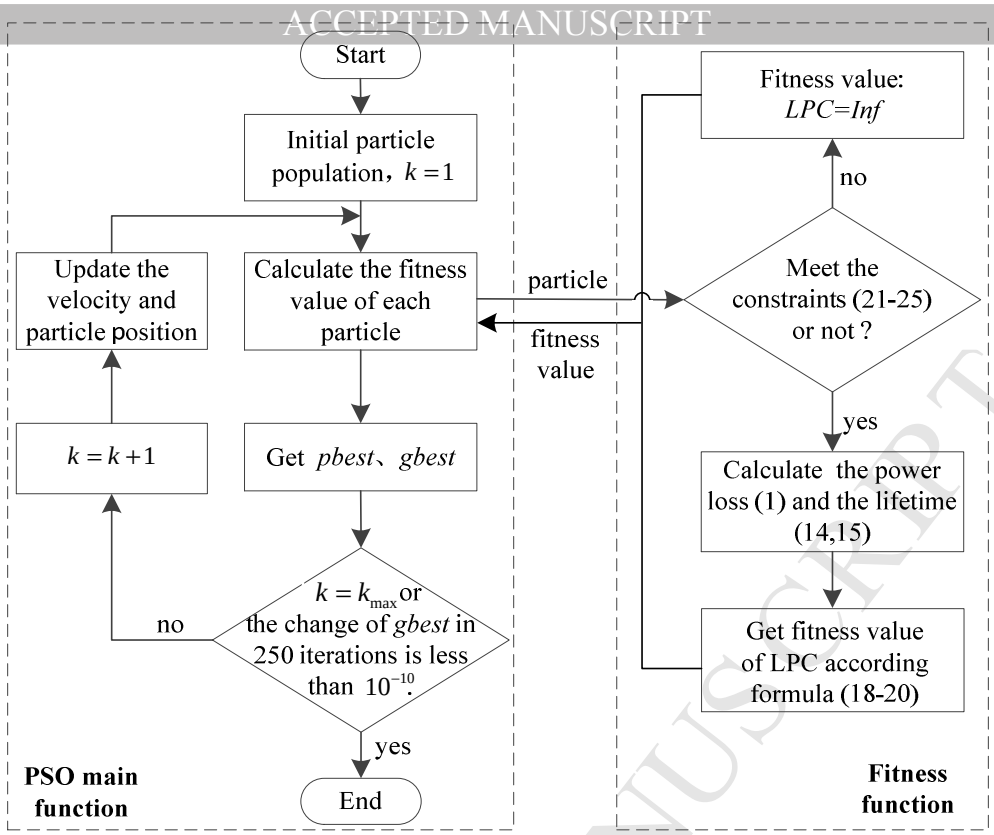

Fig. 3. *Particle Swarm Optimisation algorithm flow chart.*

Fig. 3 contains two parts: the PSO main function, and the fitness function. When the PSO main function produces a generation of particles, each particle is fed into the fitness function. First, it is judged whether the particle satisfies the constraints. If the constraints are not satisfied, the objective function value, LPC, is directly infinite. If the constraints are satisfied, the power loss and the lifetime are calculated by Equations (13)–(15), and then the LPC is calculated by Equation (17). Then, the fitness value of each particle is returned to the main function for comparison and updating, and obtaining the next generation of particles. The iteration process continues in this way until the termination condition is met.

5. Case Study

This section presents the results of a WT lifetime calculation. In addition, the proposed strategy and a traditional proportional dispatch strategy (from [10]) are compared in a WF under different scenarios. The WF model chosen for the simulation consists of 25 WTs arranged in 5 rows and 5 columns, as shown in Fig. 4. The parameters of the WTs are listed in Table I. The distance between two WTs is 882 m. The parameters of the cables are listed in Table II, in which three specifications have been adopted for the cables to suit different loadings.

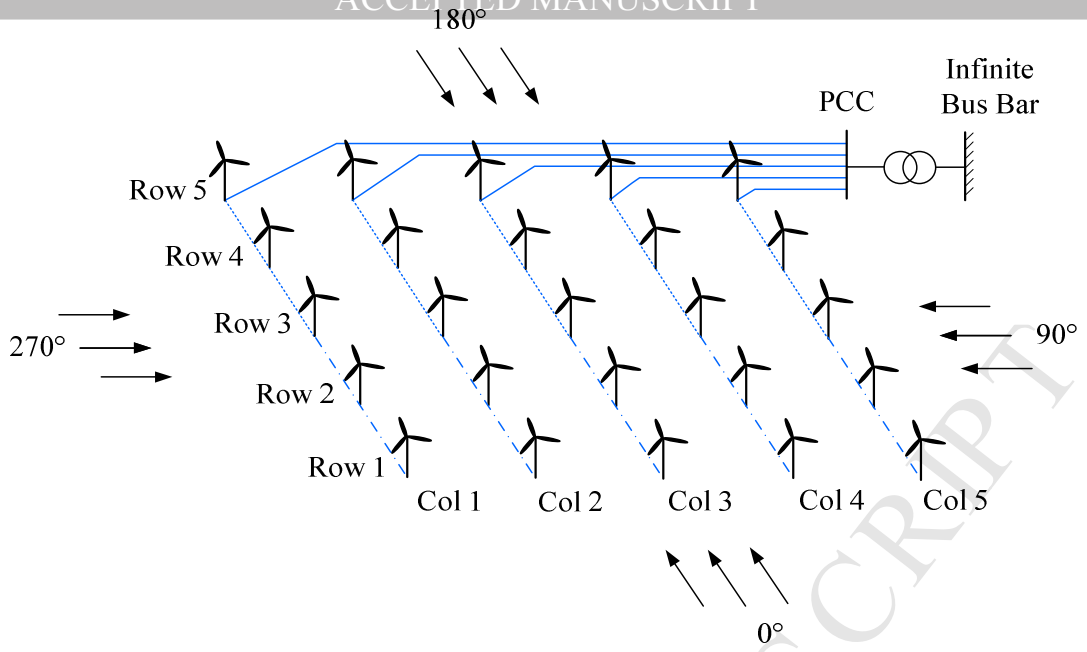

Fig. 4. *Layout of the wind farm (WF) for optimisation*

Table I Parameters of wind turbine used for optimisation [44]

Parameter	5 MW National Renewable Energy Laboratory (NREL) Wind Turbine
Cut-in, Rated, Cut-out Wind Speed	4 m/s, 11.4 m/s, 25 m/s
Rotor, Hub Diameter	126 m, 3 m
Rated Power	5 MW
Cut-In, Rated Rotor Speed	6.9 rpm, 12.1 rpm

Table II Parameters of cable used in the wind farm [45]

Cables' position	Cross section (mm^2)	Resistance (Ω/km)	Capacitance (μF/km)	Inductance (mH/km)
Row 1 - 3	95	0.1842	0.18	0.44
Row 3 - 5	150	0.1167	0.21	0.41
Row 5 - point of common coupling (PCC)	240	0.0729	0.24	0.38

5.1. Lifetime of Wind Turbine (WT)

Using the analysis in Section III and the parameters of the 5 MW NREL PMSG WT, the lifetime of the WT can be calculated. From Fig. 5, the lifetime of a WT with a specific active power and reactive power can be found. As shown in Fig. 5, when the active power remains constant, the lifetime of the WT decreases as the absolute value of the reactive power increases. As the additional reactive power causes higher thermal stress, the lifetime of the WT will be lower. Using this phenomenon, this study optimises the reactive power reference of each WT to improve the lifetime of the whole WF.

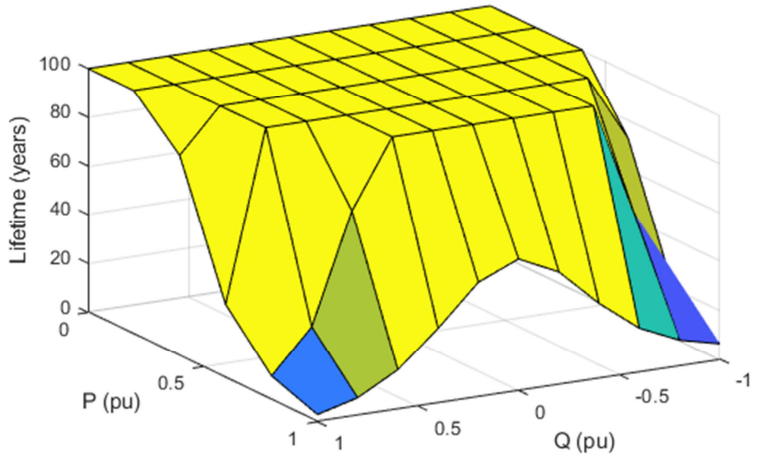

Fig. 5. *Lifetime of the wind turbine (WT)*

5.2. Case 1: Simulation at different wind velocities

As an active power dispatch strategy is out of scope of this study, a traditional maximum power point tracking (MPPT) method is adopted for the WTs. In this study, the Jensen wake model is used to calculate the active power of each WT [46]. This case presents simulation results at three different wind velocities: 6 m/s, 12 m/s, and 18 m/s. Moreover, the wind direction of the incoming wind is set to 270°, and the required reactive power reference from the grid is 0.33 p.u. As the global optimal solution of the PSO algorithm has a certain randomness, each simulation result in this study is calculated 10 times with different initial values, and the optimal result from the 10 results is taken as the final result.

(1) Scenario 1: Wind velocity = 6 m/s, wind direction = 270°, $Q_{WF}^{ref} = 0.33$

The comparisons of the traditional strategy and the proposed strategy are shown in Fig. 6, which depicts the active power, reactive power, and lifetime of all of the WTs. Table 3 shows the simulation results for Scenario 1.

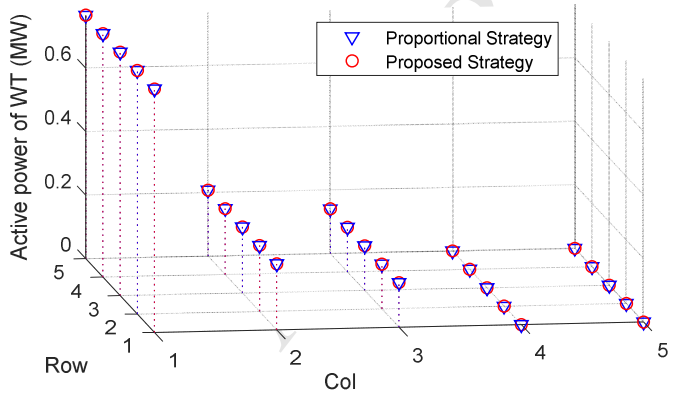

(a) Active power of WTs

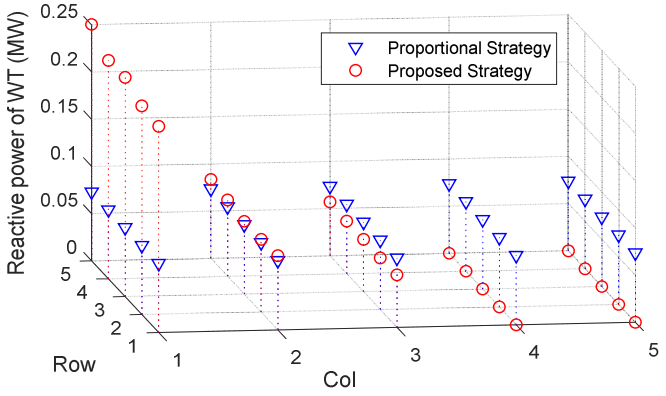

(b) Reactive power of WTs

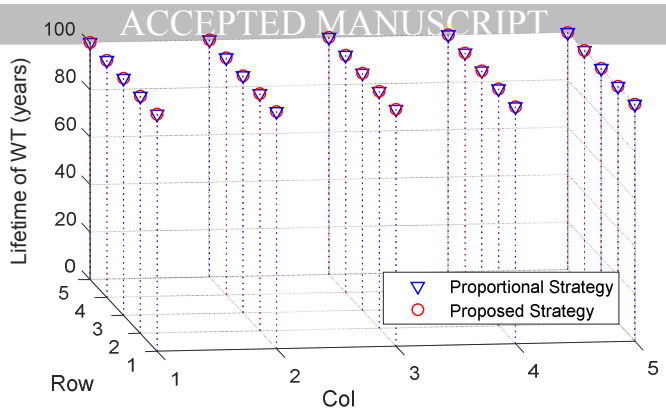

(c) Lifetime of WTs

Fig. 6*. The active power, reactive power and lifetime of WTs at Scenario 1.*

Table III Simulation result at Scenario 1 using different strategies

Strategy	Total captured power of WF (MW)	Total power loss of WF (MW)	Lifetime of WF (year)	Levelised production cost (LPC) (DKK /kWh)
Proportional strategy	5.57	0.41	100.00	110167.12
Proposed strategy	5.57	0.40	100.00	110042.95
Reduction	0	0.01	0	124.17

Table III shows that the LPC of the WF using the proposed strategy is 124.17 DKK/kWh lower than that of the proportional strategy. The lifetime of a WF is 100 years in both reactive power strategies. This is because in this scenario, the wind velocity is low, and the active powers of WTs are low, as shown in Fig. 6(a). According to Fig. 5, the lifetime of a WT with a low active power always reaches the upper limit, provided the reactive power changes within a certain range. Thus, the lifetime of WTs using the two strategies are both 100 years, as seen in Fig. 6(c). Thus, in this scenario, the LPC reduction mainly comes from the power loss reduction. The simulation result in Fig. 6(b) indicates that a higher active power with a higher reactive power of the WT will result in a smaller total loss for the WF. This phenomenon is related to the loss model formula in Section II. The mathematical calculations show that if the total reactive power of the WF is certain, then the greater reactive power allocated to the larger active power will make the sum of the square roots of the active and reactive power of all of the WTs smaller. A large part of the total loss of the WF is proportional to the square root of the active and reactive power of the WT, leading to the optimisation results shown in Fig. 6(b). In summary, when the wind velocity is low, the main optimisation object of the proposed strategy is the total loss of the WF.

(2) Scenario 2: Wind velocity = 12 m/s, wind direction = 270°, $Q_{WF}^{ref} = 0.33$

Comparisons of the proportional strategy and the proposed strategy are shown in Fig. 7, where the active power, reactive power, and lifetime of all of the WTs can be observed. Table IV presents the simulation results of Scenario 2.

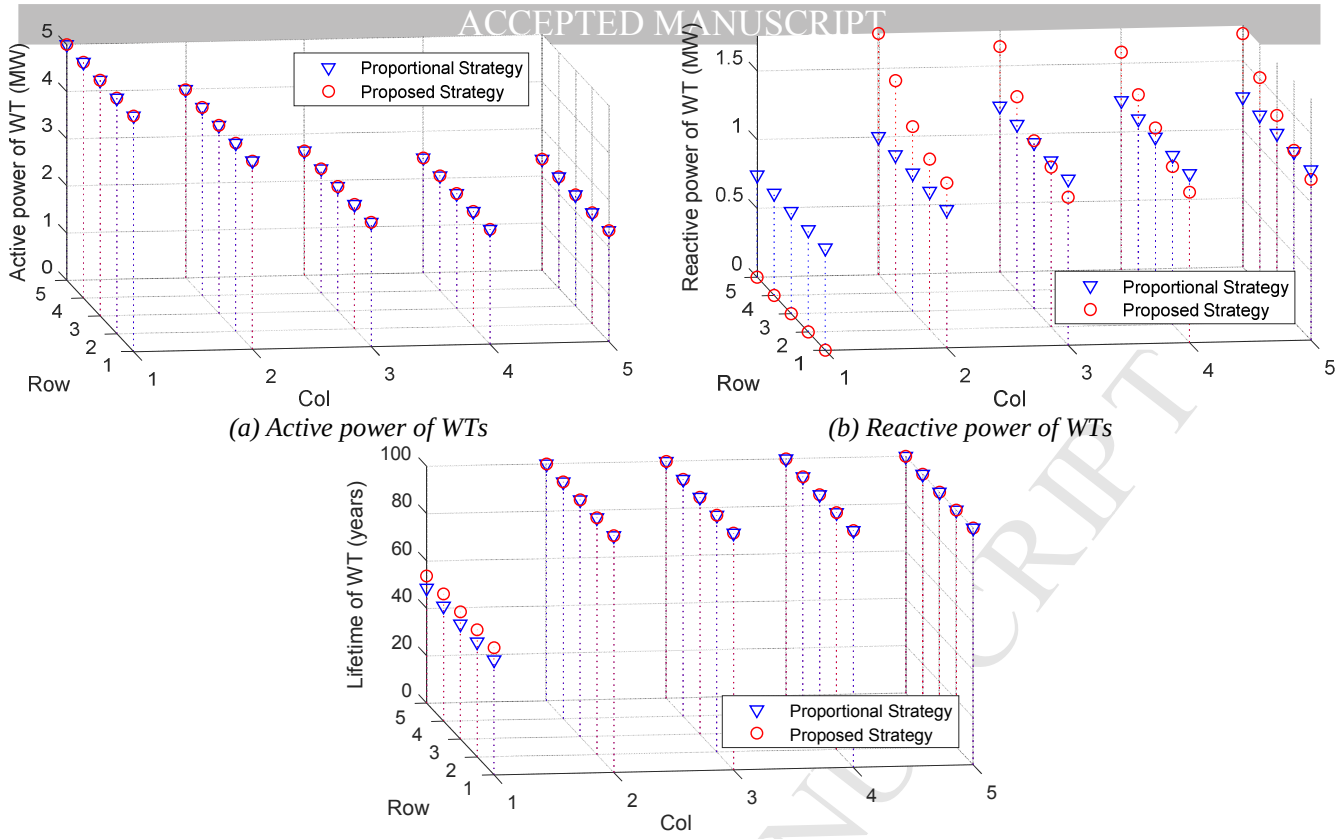

(a) Active power of WTs *(b) Reactive power of WTs*

(c) Lifetime of WTs

Fig. 7 *Active power, reactive power, and lifetime of WTs in Scenario 2.*

Table IV Simulation results of Scenario 2 using two different strategies

Strategy	Total captured power of WF (MW)	Total power loss of WF (MW)	Lifetime of WF (year)	LPC (DKK /kWh)
Proportional strategy	82.11	1.81	48.55	7752.34
Proposed strategy	82.11	1.83	53.68	7580.97
Reduction	0	-0.02	-5.13	171.37

In Table IV, the LPC of the WF using the proposed strategy is 171.37 DKK/kWh lower than that of the proportional strategy. In this scenario, the lifetime of the WF can be greatly improved by using the proposed strategy. As shown in Fig. 7, the lifetime of WTs in Column 1 is 48.55 years using the proportional strategy. While using the proposed strategy, the WTs in Column 1 are assigned to give lower reactive power, because they generate higher active power. Thus their lifetime increases to 53.68 years. As the active power of the WTs at Columns 2 to 5 are low, they have a larger threshold to generate reactive power, while still maintaining the lifetime of 100 years. Thus, the reactive power of the WTs at Columns 2 to 5 can be higher, to offset the lower reactive power of the WTs in Column 1. As a cost of obtaining a longer lifetime, the total loss of the WF increases. The total loss of the WF y using the proposed strategy is 0.02 MW higher than that of the proportional strategy. However, its growth has less impact on the LPC

minimisation than the lifetime increasing, so the optimisation of the LPC is still very evident. In summary, when the wind velocity is at a suitable value in a middle area, the proposed method mainly optimises the lifetime of a WF.

(3) Scenario 3: Simulation at: Wind velocity =18 m/s, wind direction =270°, $Q_{WF}^{ref} = 0.33$

A comparison of the proportional strategy and the proposed strategy is shown in Fig. 8, where the active power, reactive power, and lifetime of all of the WTs can be seen. Table V shows the simulation results for Scenario 3.

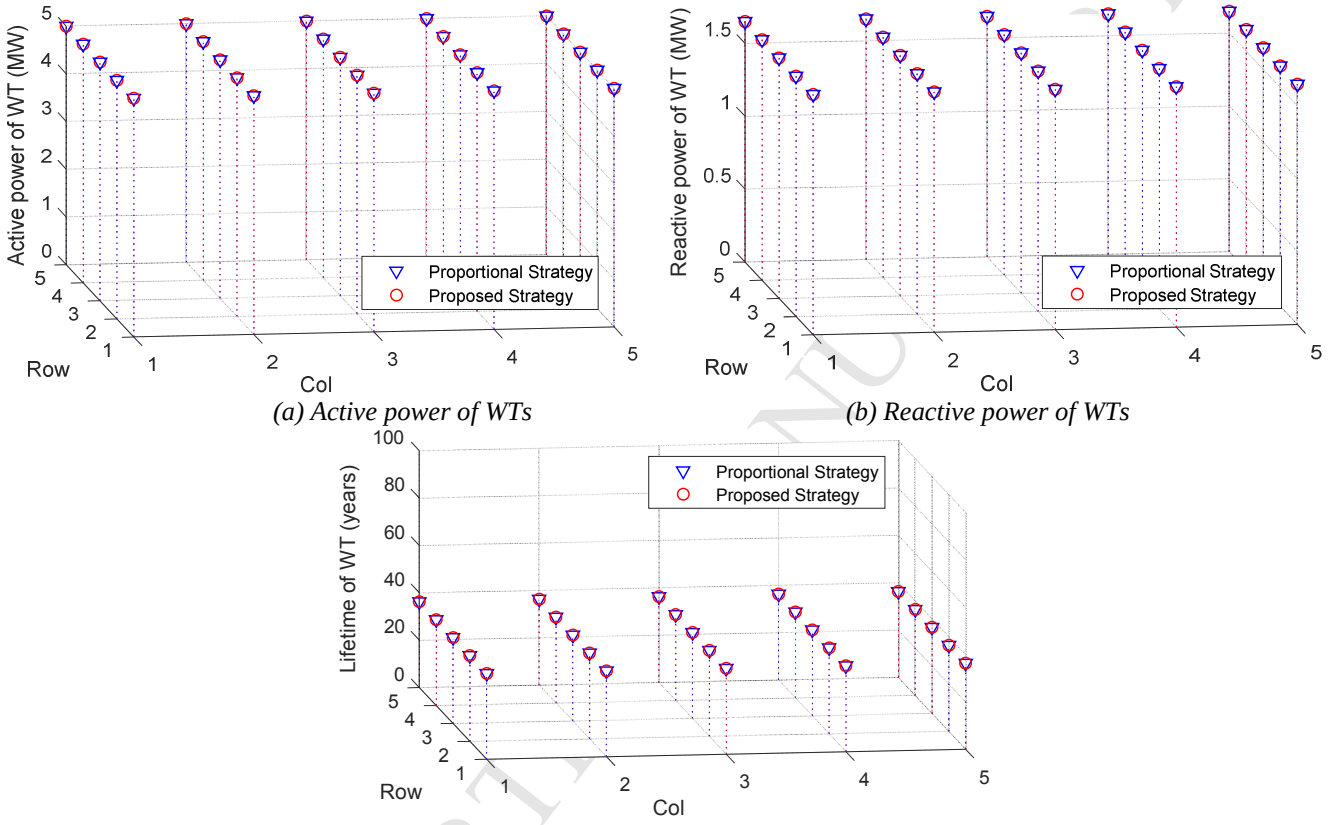

(a) Active power of WTs *(b) Reactive power of WTs*

(c) Lifetime of WTs

***Fig. 8** Active power, reactive power, and lifetime of wind turbines at Scenario 3.*

Table V Simulation result at Scenario 3 using different strategies

Strategy	Total captured power of WF (MW)	Total power loss of WF (MW)	Lifetime of WF (year)	LPC (DKK /kWh)
Proportional strategy	125.00	2.81	36.24	5568.05
Proposed strategy	125.00	2.81	36.25	5567.69
Reduction	0	0.00	-0.01	0.35

In Table V, the LPC of the WF using the proposed strategy is 0.35 DKK/kWh lower than that of the proportional strategy, which is a small number. In this scenario, the wind velocity is large enough that the output of each WT reaches a maximum of 5 MW. All of the WTs do not have a large enough margin to

regulate the reactive power. Thus, the LPC reduction is small.

(4) Scenario 4: Simulation at different wind velocities

In addition, all wind speeds from 4 m/s to 25 m/s were sampled at 1 m/s intervals to perform the simulation. Using the Jensen model, the active powers captured by the WF and the LPCs of the WF under different wind velocities are shown in Fig. 9 and Fig. 10, respectively.

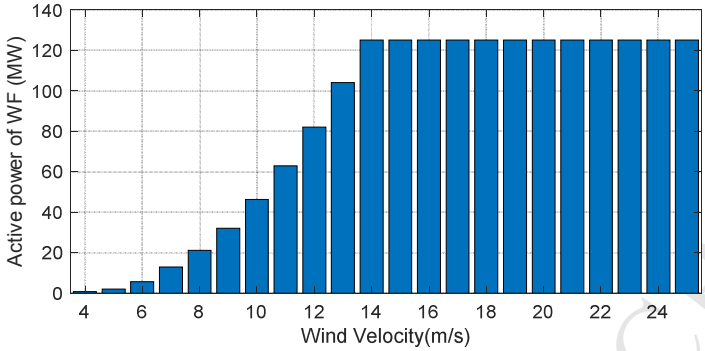

Fig. 9 *Active power captured by the wind farm for different wind speeds*

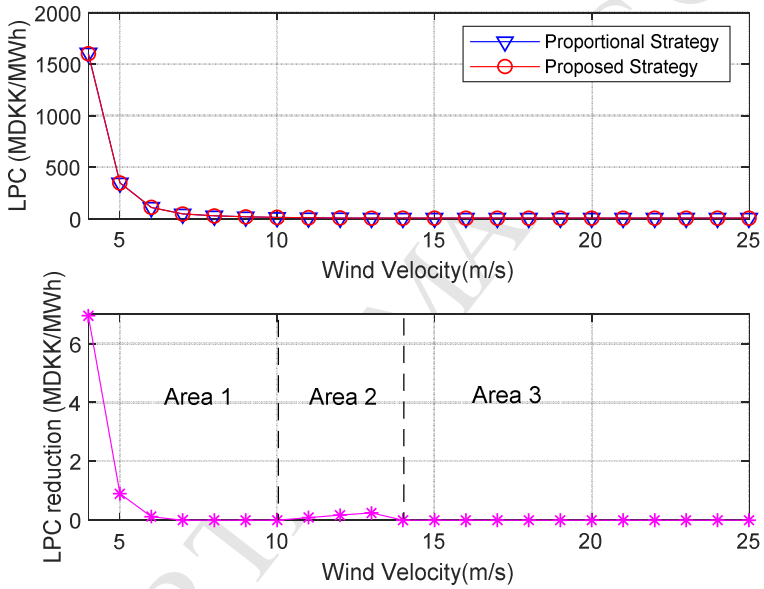

Fig. 10 *Levelised production cost (LPC) of the wind farm and LPC reduction for different wind speeds*

As shown in Fig. 9 and Fig. 10, the downward trend of the LPC is similar to the upward trend of the active power of the WF. This is because the LPC is inversely proportional to the active power of WF, as can be seen from Equation (21). The LPC reduction shown in Fig. 10 can be separated into three areas. In Area 1, when the wind velocity is below 10 m/s, the main contribution of the proposed strategy is minimising the total loss of the WF, as in Scenario 1. This contribution will be amplified as the total captured power decreases. This explains why the downward trend of LPC reduction is similar to the upward trend of the active power of the WF in Area 1. In Area 2, when the wind velocity is between 10 m/s and 14 m/s, the proposed method mainly optimises the lifetime of the WF as in Scenario 2. In this area, some but not all of the WTs have reached their maximum output. This situation creates favourable

conditions for optimising the lifetimes by assigning a lower reactive power to the WTs that reach the maximum active power output, leaving the remaining WTs to take over more reactive power. Thus, the lifetime of the WF can be significantly improved, and the LPC reduction is more evident in Area 2. In Area 3, when the wind velocity is higher than 14 m/s, the LPC reduction is almost zero, as in Scenario 3. This is because the wind velocity is large enough that the output of each WT reaches a maximum of 5 MW. All of the WTs do not have a large enough margin to regulate the reactive power, and thus the LPC reduction is small in Area 3.

5.3. Case II：Simulation of a year

To evaluate the effectiveness of the proposed strategy more comprehensively, it is necessary to simulate over a course of a year. Fig. 11 shows a wind rose that reflects the wind velocity and wind direction in a year. The wind data is obtained from the NREL National Wind Technology Centre [47] and was sampled every 3 h, totalling 2920 pieces of data. Assuming that the WF reactive power reference from the grid is normally distributed, the values and their times of appearance are shown in Fig. 12. The sum of appearance times at each value is 2920, and aims to match the data of wind velocity and wind direction.

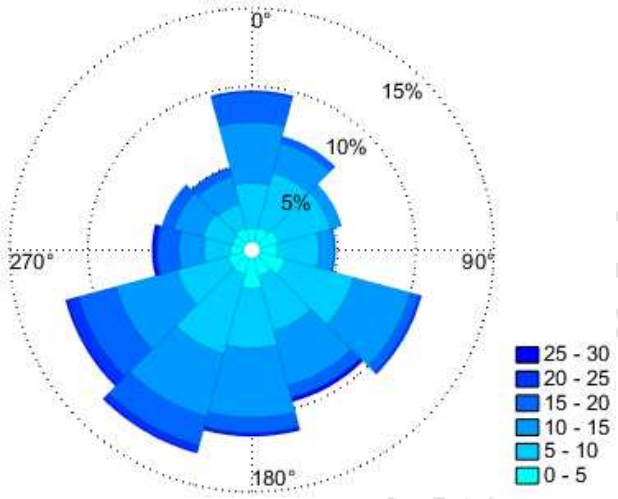

Fig. 11 *Wind rose of a year for case study (m/s).*

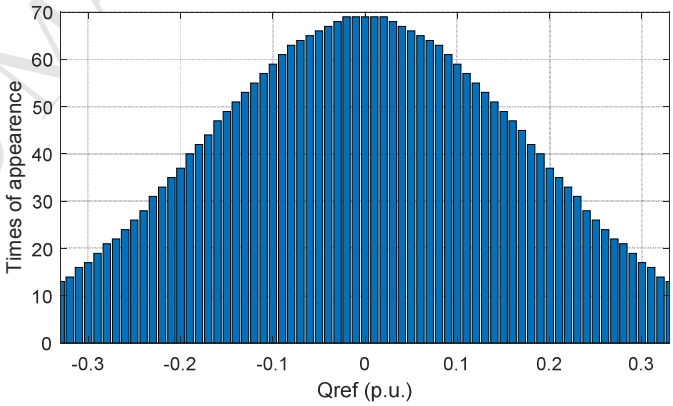

Fig. 12. *A year's* Q_{WF}^{ref} *in pu.*

The LPC of the WF using the proportional strategy and the proposed strategy is compared for one year. The total captured power of the WF, the total loss of the WF, the lifetime of the WF and the LPC are listed in Table VI.

Table VI Simulation result of a year

Strategy	Total captured power of WF (GWh)	Total power loss of WF (GWh)	Lifetime of WF (year)	LPC (DKK /kWh)
Proportional strategy	606.44	13.19	70.57	8607.32
Proposed strategy	606.44	13.19	70.84	8603.73

Reduction	0	-0.01	-0.27	3.59

As the active power dispatch of the WF is the same in these two strategies, the total captured power of the WF in a year for both these two strategies is 606.44 GWh. The total power loss of the WF in a year of the proposed strategy is 0.01 GWh higher than that of the proportional strategy, and is the price of lifetime optimisation. Table VI shows that the WF can operate for 70.84 years using the proposed strategy, 0.27 years longer than that of the proportional strategy. As a result, the LPC of the WF using the proposed strategy is 3.59 DKK/kWh smaller than that of the traditional strategy.

In fact, the lifetime of a WT is usually 20 to 25 years, i.e. much shorter than the 70.84 years mentioned above. However, the lifetime calculated in this study can reflect the fatigue of the converter. Extending the lifetime of the converter can effectively reduce the frequency and cost of maintenance of the converter.

6. Conclusions

In this paper, a reactive power dispatch strategy is proposed to minimise the LPC of a WF. This goal is achieved in two ways: minimising the power loss of the WF, and maximising the lifetime of WTs. Considering the wake effect in a WF, the upstream WTs generate higher active power, which generally causes a shorter lifetime. For these WTs, using the proposed method to reduce their reactive power reference can effectively increase their lifetime. For the downstream WTs with lower generated active power, they have enough capacity to provide more reactive power, and their lifetime will never be shorter than the industrial standard. Consequently, for downstream WTs, the main task of the proposed method is to find the appropriate reactive power reference of the WTs to minimise the power loss of the WF. Furthermore, in the case of a year, the LPC of the WF using the proposed strategy is 3.59 DKK/kWh smaller than that of the traditional strategy, meaning the proposed strategy has higher economic benefits.

In future study, as the active power dispatch has a great impact on the WF productivity and the lifetime of WTs, the active power and reactive power of WTs will both be considered as the optimisation objects to minimise the LPC of the WF.

7. Acknowledgment

This work was supported by the National Natural Science Foundation of China (51707029) and the National Key Research and Development Program of China (2017YFB0902000).

8. References

[1] Global Wind Energy Council. Global Wind Report 2018. Available online: https://gwec.net/wp-content/uploads/2019/04/GWEC-Global-Wind-Report-2018.pdf.

[2] Global Wind Energy Council. Global Wind Report 2017. Available online: http://gwec.net/cost-competitiveness-puts-wind-in-front/

[3] Du E, Zhang N, Kang C, et al. Managing wind power uncertainty through strategic reserve purchasing. IEEE Transactions on Power Systems, 2017, 32(4): 2547-2559.

[4] Dvorkin Y, Lubin M, Backhaus S, et al. Uncertainty sets for wind power generation. IEEE Transactions on Power Systems, 2016, 31(4): 3326-3327.

[5] Sadeghfam A, Tohidi S, Rostami N. Influence of PMSG‐based wind turbine on transient stability of synchronous generators—a comparative study. International Transactions on Electrical Energy Systems, 2018, 28(12): e2639.

[6] Ajami A, Armaghan M. Fixed speed wind farm operation improvement using current-source converter based UPQC. Energy conversion and management, 2012, 58: 10-18.

[7] Bensmaine F, Bachelier O, Tnani S, et al. LMI approach of state-feedback controller design for a STATCOM-supercapacitors energy storage system associated with a wind generation. Energy conversion and management, 2015, 96: 463-472.

[8] Weng Y T, Hsu Y Y. Reactive power control strategy for a wind farm with DFIG. Renewable energy, 2016, 94: 383-390.

[9] Ghennam T, Aliouane K, Akel F, et al. Advanced control system of DFIG based wind generators for reactive power production and integration in a wind farm dispatching. Energy Conversion and Management, 2015, 105: 240-250.

[10] Tapia G, Tapia A, Ostolaza J X. Proportional–integral regulator-based approach to wind farm reactive power management for secondary voltage control. IEEE Transactions on Energy Conversion, 2007, 22(2): 488-498.

[11] Mohseni-Bonab S M, Rabiee A. Optimal reactive power dispatch: a review, and a new stochastic voltage stability constrained multi-objective model at the presence of uncertain wind power generation. IET Generation, Transmission & Distribution, 2017, 11(4): 815-829.

[12] Mohseni-Bonab S M, Rabiee A, Mohammadi-Ivatloo B. Voltage stability constrained multi-objective optimal reactive power dispatch under load and wind power uncertainties: A stochastic approach. Renewable Energy, 2016, 85: 598-609.

[13] Zhang B, Hou P, Hu W, et al. A reactive power dispatch strategy with loss minimization for a DFIG-based wind farm. IEEE Transactions on Sustainable Energy, 2016, 7(3): 914-923.

[14] Ou R, Xiao X Y, Zou Z C, et al. Cooperative control of SFCL and reactive power for improving the transient voltage stability of grid-connected wind farm with DFIGs. IEEE Transactions on Applied Superconductivity, 2016, 26(7): 1-6.

[15] Zeng X, Yao J, Chen Z, et al. Co-ordinated control strategy for hybrid wind farms with PMSG and FSIG under unbalanced grid voltage condition. IEEE Transactions on Sustainable Energy, 2016, 7(3): 1100-1110.

[16] Agalar S, Kaplan Y A. Power quality improvement using STS and DVR in wind energy system. Renewable energy, 2018, 118: 1031-1040.

[17] Rather Z H, Chen Z, Thøgersen P, et al. Dynamic reactive power compensation of large-scale wind integrated power system. IEEE Transactions on Power Systems, 2015, 30(5): 2516-2526.

[18] Li Q, Zhang Y, Ji T, et al. Volt/Var control for power grids with connections of large-scale wind farms: A review. IEEE Access, 2018, 6: 26675-26692.

[19] Ouyang J, Li M, Diao Y, et al. Active control method of large-scale wind integrated power system with enhanced reactive power support for wind speed fluctuation. IET Generation, Transmission & Distribution, 2018, 12(21): 5664-5671.

[20] Ouyang J, Li M, Zhang Z, et al. Multi-Timescale Active and Reactive Power-Coordinated Control of Large-Scale Wind Integrated Power System for Severe Wind Speed Fluctuation. IEEE Access, 2019, 7: 51201-51210.

[21] Amaris H, Alonso M. Coordinated reactive power management in power networks with wind turbines and FACTS devices. Energy Conversion and Management, 2011, 52(7): 2575-2586.

[22] Jung S, Jang G. A loss minimization method on a reactive power supply process for wind farm. IEEE Transactions on Power Systems, 2017, 32(4): 3060-3068.

[23] He J, Li Q, Ma J, et al. Research on capacity configuration method of concentrated reactive power compensator for wind farm LVRT capability. The Journal of Engineering, 2017, 2017(13): 2428-2432.

[24] Weng Y T, Hsu Y Y. Reactive power control strategy for a wind farm with DFIG. Renewable energy, 2016, 94: 383-390.

[25] Alonso M, Amaris H, Alvarez-Ortega C. A multiobjective approach for reactive power planning in networks with wind power generation. Renewable Energy, 2012, 37(1): 180-191.

[26] Tian J, Zhou D, Su C, et al. Reactive power dispatch method in wind farms to improve the lifetime of power converter considering wake effect. IEEE Transactions on Sustainable Energy, 2017, 8(2): 477-487.

[27] Wang N, Li J, Hu W, et al. Optimal reactive power dispatch of a full-scale converter based wind farm considering loss minimization. Renewable Energy, 2019, 139: 292-301.

[28] Villena-Ruiz R, Ramirez F J, Honrubia-Escribano A, et al. A techno-economic analysis of a real wind farm repowering experience: The Malpica case. Energy conversion and management, 2018, 172: 182-199.

[29] Nguyen T A T, Chou S Y. Maintenance strategy selection for improving cost-effectiveness of offshore wind systems. Energy conversion and management, 2018, 157: 86-95.

[30] Zhou D, Blaabjerg F, Lau M, et al. Optimized reactive power flow of DFIG power converters for better reliability performance considering grid codes. IEEE Transactions on Industrial Electronics, 2015, 62(3): 1552-1562.

[31] Li H, Chen Z. Overview of different wind generator systems and their comparisons. IET Renewable Power Generation, 2008, 2(2): 123-138.

[32] Kaempf E, Braun M. Models of reactive power ‐ related wind park losses for application in power system load flow studies. Wind Energy, 2017, 20(7): 1291-1309.

[33] Zhang B, Hu W, Hou P, et al. Coordinated power dispatch of a PMSG based wind farm for output power maximizing considering the wake effect and losses. 2016 IEEE Power and Energy Society General Meeting (PESGM). IEEE, 2016: 1-5.

[34] Chinchilla M, Arnaltes S, Burgos J C. Control of permanent-magnet generators applied to variable-speed wind-energy systems connected to the grid. IEEE Transactions on energy conversion, 2006, 21(1): 130-135.

[35] Roshanfekr P, Thiringer T, Lundmark S, et al. Selecting IGBT module for a high voltage 5 MW wind turbine PMSG-equipped generating system. 2012 IEEE Power Electronics and Machines in Wind Applications. IEEE, 2012: 1-6.

[36] Petersson A. Analysis, modeling and control of doubly-fed induction generators for wind turbines. Chalmers University of Technology, 2005.

[37] Saadat H. Power system analysis[M]. 1999, pp. 189–219.

[38] Zhou D, Wang H, Blaabjerg F. Mission profile based system-level reliability analysis of DC/DC converters for a backup power application. IEEE Transactions on Power Electronics, 2018, 33(9): 8030-8039.

[39] Yao J, Pei J, Xu D, et al. Coordinated control of a hybrid wind farm with DFIG-based and PMSG-based wind power generation systems under asymmetrical grid faults. Renewable energy, 2018, 127: 613-629.

[40] Zhou D, Blaabjerg F, Franke T, et al. Comparison of wind power converter reliability with low-speed and medium-speed permanent-magnet synchronous generators. IEEE Transactions on Industrial Electronics, 2015, 62(10): 6575-6584.

[41] Lundberg S. Performance comparison of wind park configurations. Chalmers University of Technology, 2003.

[42] Kennedy J. Particle swarm optimization. Encyclopedia of machine learning, 2010: 760-766.

[43] Ajdad H, Baba Y F, Al Mers A, et al. Particle swarm optimization algorithm for optical-geometric optimization of linear fresnel solar concentrators. Renewable energy, 2019, 130: 992-1001.

[44] Jonkman J, Butterfield S, Musial W, et al. Definition of a 5-MW reference wind turbine for offshore system development. National Renewable Energy Lab (NREL), Golden, CO (United States), 2009.

[45] ABB. XLPE Submarine Cable Systems. Online: http://www05.abb.com/global/scot/scot245.nsf/veritydisplay/2fb0094306e48975c125777c00334767/$file/XLPE%20Submarine%20Cable%20Systems%202GM5007%20rev%205.pdf

[46] González-Longatt F, Wall P, Terzija V. Wake effect in wind farm performance: Steady-state and dynamic behavior. Renewable Energy, 2012, 39(1): 329-338.

[47] NREL National Wind Technology Center, 2017 Available online: https://midcdmz.nrel.gov/apps/go2url.pl?site=NWTC

Highlights:

(1) An optimal reactive power dispatch of wind farm is proposed to minimize the LPC.

(2) The power loss and lifetime of wind farm are both considered in the optimal strategy.

(3) The LPC of proposed strategy is 3.59 DKK/kWh smaller than traditional strategy.